Proceedings of DETC'03
2003 ASME Design Engineering Technical Conferences and
Computer and Information in Engineering Conference
September 2-6, 2003, Chicago, Illinois, USA

DETC03/VIB48432

CONSTRAINT STABILIZATION FOR TIME-STEPPING APPROACHES FOR RIGID MULTIBODY DYNAMICS WITH JOINTS, CONTACT, AND FRICTION

Mihai Anitescu *
Mathematics and Computer Science Division,
Building 221, Argonne National Laboratory,
9700 South Cass Avenue,
Argonne, IL 60439, U.S.A
email: anitescu@mcs.anl.gov

Andrew Miller
Dept. of Computer Science
Columbia University
New York, NY 10027, USA

Gary D. Hart
Department of Mathematics,
University of Pittsburgh
Pittsburgh, PA 15260, USA

ABSTRACT

We present a method for achieving geometrical constraint stabilization for a linear-complementarity-based time-stepping scheme for rigid multibody dynamics with joints, contact, and friction. The method requires the solution of only one linear complementarity problem per step. The method depends on an adjustable parameter γ, but the constraint stabilization effect is shown to hold for any $\gamma \in (0, 1]$. Several examples are used to demonstrate the constraint stabilization effect.

Keywords Coulomb friction, Complementarity Problem, Constraint Stabilization.

1 Introduction

Simulating the dynamics of a system with several rigid bodies and with joint, contact (noninterpenetration), and friction constraints is an important part of virtual reality and robotics simulations.

If the simulation has only joint constraints, then the problem is a differential algebraic equation (DAE) (Haug, 1989; Ascher and Petzold, 1998). However, the nonsmooth nature of the noninterpenetration and friction constraints requires the use of specialized techniques. Approaches used in the past for simulating rigid multibody dynamics with contact and friction include piecewise DAE approaches (Haug, 1989), acceleration-force linear complementarity problem (LCP) approaches (Glocker and Pfeiffer, 1992; Baraff, 1993; Lo et al., 1997), penalty (or regularization) approaches (Donald and Pai, 1990; Song et al., 2001), and velocity-impulse LCP-based time-stepping methods (Stewart and Trinkle, 1995; Stewart, 2000; Anitescu and Potra, 1997; Anitescu et al., 1999). When the value of the timestep is set to 0, the LCP of the velocity-impulse approach is the same as the one used in the compression phase of multiple collision resolution (Glocker and Pfeiffer, 1995).

Of all these approaches the penalty approach is probably the most encountered mechanical engineering literature. It accommodates the nonsmooth nature of contact and friction by smoothing their mathematical descriptions. The advantage of this approach is that it is easy to set up and results in a DAE, for which both analytical and software tools are in a fairly mature state of development. The disadvantages are that apriory finding appropriate values for the smoothing parameters is difficult and that it results a very stiff problem even for moderate time steps.

The LCP method represents both contact and friction as inequality constraints that are computationally treated as hard constraints. The advantage of this method is that there are no extra parameters to tune and no artificial stiffness. It may therefore be expected to work better with less user input. On the other hand, the subproblems are now constrained by inequalities, and separate analysis and software tools need to be developed to make the approach successfull.

In this work we use the velocity-impulse LCP-based approach, which has the advantage that it does not suffer from the lack of a solution that can appear the piecewise DAE and

*Address all correspondence to this author

acceleration-force LCP approach (Baraff, 1993; Stewart, 2000). It also does not suffer from the artificial stiffness that is introduced by the penalty approach. In previous work, we have shown how to approach stiffness (Anitescu and Potra, 2002) and constraint stabilization (Anitescu and Hart, 2002).

In this work we analyze an extension of the method in (Anitescu and Hart, 2002) to achieve geometrical (noninterpenetration and joint) constraint stabilization for complementarity-based time-stepping methods for rigid multibody dynamics with contact, joints, and friction. The scheme we analyze here is currently used for the dynamical simulation of dynamical robotic grasps (Miller and Christensen, 2002). This scheme needs no computational effort other than that for solving the basic LCP subproblem, though the free term of the LCP is modified compared with other time-stepping LCP approaches (Anitescu and Potra, 2002; Anitescu and Potra, 1997; Stewart and Trinkle, 1995).

The constraint stabilization issue in a complementarity setting has been tackled by using nonlinear complementarity problems (Stewart and Trinkle, 1995), an LCP followed by a nonlinear projection approach that includes nonlinear inequality constraints (Anitescu and Potra, 2002), and a postprocessing method (Cline 2002) that uses one potentially nonconvex LCP based on the stiff method developed in (Anitescu and Potra, 2002) followed by one convex LCP for constraint stabilization. When applied to joint-only systems, the method from (Cline 2002) belongs to the set of postprocessing methods defined in (Ascher et al., 1994; Ascher et al., 1995). In order to achieve constraint stabilization, however, all of these methods need additional computation after the basic LCP subproblem has been solved. This stands in contrast with this approach that needs no additional computational effort to achieve constraint stabilization.

2 The Linear Complementarity Subproblem of the Time-Stepping Scheme

In this section, we review a velocity-impulse LCP-based time-stepping scheme that uses an Euler discretization (Anitescu and Potra, 1997; Stewart and Trinkle, 1995). In the following, q and v constitute, respectively, the generalized position and generalized velocity vector of a system of several bodies (Haug, 1989).

2.1 Model Constraints

Throughout this subsection we use **complementarity notation**. If $a,b \in IR$, we say that a is complementary to b, and we denote it by $a \perp b$ or $a \geq 0 \perp b \geq 0$ if $a \geq 0$, $b \geq 0$, and $ab = 0$.

2.1.1 Geometrical Constraints Joint constraints (2.1) and noninterpenetration constraints (2.3) involve only the position variable and depend on the shape of the bodies and the type of constraints involved. We call them geometrical constraints.

Joint Constraints. Joint constraints are described by the equations

$$\Theta^{(i)}(q) = 0,\ i = 1,2,\ldots,m. \tag{2.1}$$

Here, $\Theta^{(i)}(q)$ are sufficiently smooth functions. We denote by $\nu^{(i)}(q)$ the gradient of the corresponding function, or

$$\nu^{(i)}(q) = \nabla_q \Theta^{(i)}(q), \quad i = 1,2,\ldots,m. \tag{2.2}$$

The impulse exerted by a joint on the system is $c_\nu^{(i)} \nu^{(i)}(q)$, where $c_\nu^{(i)}$ is a scalar related to the Lagrange multiplier of classical constrained dynamics (Haug, 1989).

Noninterpenetration Constraints. Noninterpenetration constraints are defined in terms of a continuous signed distance function between the two bodies $\Phi^{(j)}(q)$ (Anitescu et al., 1996). The noninterpenetration constraints become

$$\Phi^{(j)}(q) \geq 0, \quad j = 1,2,\ldots,p. \tag{2.3}$$

The function $\Phi^{(j)}(q)$ is generally not differentiable everywhere. We discuss sufficient conditions for local differentiability of $\Phi^{(j)}(q)$ in (Anitescu and Hart, 2002). In the following, we refer to j as the *contact* j, although the contact is truly active only when $\Phi^{(j)}(q) = 0$. We denote the normal at contact (j) by

$$n^{(j)}(q) = \nabla_q \Phi^{(j)}(q), \quad j = 1,2,\ldots,p. \tag{2.4}$$

When the contact is active, it can exert a compressive normal impulse, $c_n^{(j)} n^{(j)}(q)$, on the system, which is quantified by requiring $c_n^{(j)} \geq 0$. The fact that the contact must be active before a nonzero compression impulse can act is expressed by the complementarity constraint

$$\Phi^{(j)}(q) \geq 0 \perp c_n^{(j)} \geq 0, \quad j = 1,2,\ldots,p. \tag{2.5}$$

Differentiability properties. The mappings $\Theta^{(i)}(q)$ that define the joint constraints are differentiable (Haug, 1989). The situation, is different, however, for the mapping defining the noninterpenetration constraints. The mappings $\Phi^{(j)}(q)$ cannot be differentiable everywhere, in general, no matter how simple or regular the shape of the bodies (Anitescu and Hart, 2002). If the bodies are smooth and relatively strictly convex, then the mapping $\Phi^{(j)}(q)$ is differentiable as long as the interpenetration value is

not large (Anitescu et al., 1996). The mappings $\Phi^{(j)}(q)$ are obviously not differentiable for bodies with nonsmooth shapes.

To simplify our analysis, we assume that the mappings that define the joint and noninterpenetration constraints are differentiable. If the shapes are such that the mappings $\Phi^{(j)}(q)$ are differentiable only for small values of the interpenetration, then the analysis of this work can be extended, in a straightforward though laborious manner, as in (Anitescu and Hart, 2002) to demonstrate the constraint stabilization effect.

Since any body can be approximated by a finite union of convex, smooth-shaped bodies, we could extend, in principle, the analysis in this work for approximation of any configuration. Probably, however, it is computationally more efficient to accommodate nonsmooth or nonconvex shapes directly, by working with a piecewise smooth mapping $\Phi^{(j)}$. We defer the analysis of this situation to future research.

2.1.2 Frictional Constraints Frictional constraints are expressed by means of a discretization of the Coulomb friction cone (Anitescu and Potra, 2002; Anitescu and Potra, 1997; Stewart and Trinkle, 1995). For a contact $j \in \{1,2,\ldots,p\}$, we take a collection of coplanar vectors $d_i^{(j)}(q)$, $i = 1,2,\ldots,m_C^{(j)}$, which span the plane tangent at the contact (though the plane may cease to be tangent to the contact normal when mapped in generalized coordinates (Anitescu et al., 1996)). The convex cover of the vectors $d_i^{(j)}(q)$ should approximate the transversal shape of the friction cone. In two-dimensional mechanics, the tangent plane is one dimensional, its transversal shape is a segment, and only two such vectors $d_1^{(j)}(q)$ and $d_2^{(j)}(q)$ are needed in this formulation. We denote by $D^{(j)}(q)$ a matrix whose columns are $d_i^{(j)}(q) \neq 0$, $i = 1,2,\ldots,m_C^{(j)}$, that is, $D^{(j)}(q) = \left[d_1^{(j)}(q), d_2^{(j)}(q), \ldots, d_{m_C^{(j)}}^{(j)}(q)\right]$. A tangential impulse is $\sum_{i=1}^{m_C^{(j)}} \beta_i^{(j)} d_i^{(j)}(q)$, where $\beta_i^{(j)} \geq 0$, $i = 1,2,\ldots,m_C^{(j)}$. We assume that the tangential contact description is balanced, that is,

$$\forall 1 \leq i \leq m_C^{(j)},\ \exists k,\ 1 \leq k \leq m_C^{(j)} \text{ such that } d_i^{(j)}(q) = -d_k^{(j)}(q). \tag{2.6}$$

The friction model ensures maximum dissipation for given normal impulse $c_n^{(j)}$ and velocity v and guarantees that the total contact force is inside the discretized cone. We express this model as

$$\begin{aligned} D^{(j)^T}(q)v + \lambda^{(j)} e^{(j)} \geq 0 \perp \beta^{(j)} \geq 0, \\ \mu c_n^{(j)} - e^{(j)^T} \beta^{(j)} \geq 0 \perp \lambda^{(j)} \geq 0. \end{aligned} \tag{2.7}$$

Here $e^{(j)}$ is a vector of ones of dimension $m_C^{(j)}$, $e^{(j)} = (1,1,\ldots,1)^T$, $\mu^{(j)} \geq 0$ is the Coulomb friction parameter, and $\beta^{(j)}$ is the vector of tangential impulses $\beta^{(j)} = \left(\beta_1^{(j)}, \beta_2^{(j)}, \ldots, \beta_{m_C^{(j)}}^{(j)}\right)^T$. The additional variable $\lambda^{(j)} \geq 0$ is approximately equal to the norm of the tangential velocity at the contact, if there is relative motion at the contact, or $\left|\left|D(q)^{(j)^T} v\right|\right| \neq 0$ (Anitescu and Potra, 1997; Stewart and Trinkle, 1995).

Notation. We denote by $M(q)$ the symmetric, positive definite mass matrix of the system in the generalized coordinates q and by $k(t,q,v)$ the external force. All quantities described in this section associated with contact j are denoted by the superscript $^{(j)}$. When we use a vector or matrix norm whose index is not specified, it is the 2 norm.

2.2 The Linear Complementarity Problem

Let $h_l > 0$ be the time step at time $t^{(l)}$, when the system is at position $q^{(l)}$ and velocity $v^{(l)}$. We have that $h_l = t^{(l+1)} - t^{(l)}$. We choose the new position to be $q^{(l+1)} = q^{(l)} + h_l v^{(l+1)}$, where $v^{(l+1)}$ is determined by enforcing the simulation constraints.

The geometrical constraints are enforced at the velocity level by modified linearization of the mappings $\Theta^{(i)}$ and $\Phi^{(j)}$. For joint constraints the modified linearization leads to

$$\begin{aligned} \gamma\Theta^{(i)}(q^{(l)}) + h_l \nabla_q \Theta^{(i)^T}(q^{(l)}) v^{(l+1)} = \\ \gamma\Theta^{(i)}(q^{(l)}) + h_l \nu^{(i)^T}(q^{(l)}) v^{(l+1)} = 0, \quad i = 1,2,\ldots,m, \end{aligned} \tag{2.8}$$

where γ is a user-defined parameter. If $\gamma = 1$, then we would achieve proper linearization, which is the case treated in (Anitescu and Hart, 2002).

For a noninterpenetration constraint of index j, $\Phi^{(j)}(q) \geq 0$, modified linearization at $q^{(l)}$ for one time step amounts to $\gamma\Phi^{(j)}(q^{(l)}) + h_l \nabla_q \Phi^{(j)^T}(q^{(l)}) v^{(l+1)} \geq 0$; that is, after including the complementarity constraints (2.5) and using the definition of $n^{(j)}(q^{(l)})$, we have

$$n^{(j)^T}(q^{(l)}) v^{(l+1)} + \gamma \frac{\Phi^{(j)}(q^{(l)})}{h_l} \geq 0 \perp c_n^{(j)} \geq 0. \tag{2.9}$$

For computational efficiency, only the contacts that are imminently active are included in the dynamical resolution and linearized, and their set is denoted by $\mathcal{A}$. One practical way of determining $\mathcal{A}$ is by including all j for which $\Phi^{(j)}(q) \leq \hat{\varepsilon}$, where $\hat{\varepsilon}$ is a sufficiently small quantity.

The choice of $\gamma = 1$ has been analyzed in previous work (Anitescu and Hart, 2002). Although local constraint stabilization has been proved there, it is of interest to consider the case $\gamma \neq 0$ for the following reason. If we analyze the linearization of the joint constraint, we see that, to be included in a system whose unknown is $v^{(l+1)}$, it must be rewritten as

$\gamma\frac{\Theta^{(i)}(q^{(l)})}{h_l}+\mathbf{v}^{(i)^T}(q^{(l)})v^{(l+1)}=0, \quad i=1,2,\ldots,m,$. Clearly, if h_l needs to be small and $\Theta^{(i)}$ is large, this may cause a problem. So the effect of h_l being small is compensated by a suitably chosen γ. Obviously $\gamma=0$ would result in the constraint drift not being compensated at all, so some lower bound on γ is, practically speaking, necessary. As is the case with other parameter-dependent schemes, its choice in the end will be problem specific.

If a collision occurs, then a collision resolution, possibly with energy restitution, needs to be applied (Glocker and Pfeiffer, 1995; Anitescu and Potra, 1997). In our setup a collision occurs at step l for a contact j if the first inequality in (2.9) is satisfied with equality, and at step $l-1$ it was satisfied as a strict inequality.

In this work we assume that no energy lost during collision is restituted; hence we avoid the need to consider a compression LCP followed by decompression LCP (Anitescu and Potra, 1997). The relation (2.9) is sufficient to accommodate totally plastic collisions.

To completely define the LCP subproblem, we use an Euler discretization of Newton's law, which results in the following equation:

$$M(q^{(l)})\left(v^{(l+1)}-v^{(l)}\right)=h_l k\left(t^{(l)},q^{(l)},v^{(l)}\right)+\sum_{i=1}^{m}c_{\mathbf{v}}^{(i)}\mathbf{v}^{(i)}(q^{(l)})+\sum_{j\in\mathcal{A}}\left(c_n^{(j)}n^{(j)}(q^{(l)})+\sum_{i=1}^{m_c^{(j)}}\beta_i^{(j)}d_i^{(j)}(q^{(l)})\right).$$

After collecting all the constraints introduced above, with the geometrical constraints replaced by their linearized versions (2.8) and (2.9), we obtain the following mixed LCP:

$$\begin{bmatrix} M^{(l)} & -\widetilde{\mathbf{v}} & -\widetilde{n} & -\widetilde{D} & 0\\ \widetilde{\mathbf{v}}^T & 0 & 0 & 0 & 0\\ \widetilde{n}^T & 0 & 0 & 0 & 0\\ \widetilde{D}^T & 0 & 0 & 0 & \widetilde{E}\\ 0 & 0 & \widetilde{\mu} & -\widetilde{E}^T & 0 \end{bmatrix}\begin{bmatrix} v^{(l+1)}\\ c_{\mathbf{v}}\\ c_n\\ \widetilde{\beta}\\ \lambda \end{bmatrix}+\begin{bmatrix} -Mv^{(l)}-h_l k^{(l)}\\ \Upsilon\\ \Delta\\ 0\\ 0 \end{bmatrix}=\begin{bmatrix} 0\\ 0\\ \rho\\ \widetilde{\sigma}\\ \zeta \end{bmatrix} \tag{2.10}$$

$$\begin{bmatrix} c_n\\ \widetilde{\beta}\\ \lambda \end{bmatrix}^T\begin{bmatrix} \rho\\ \widetilde{\sigma}\\ \zeta \end{bmatrix}=0, \qquad \begin{bmatrix} c_n\\ \widetilde{\beta}\\ \lambda \end{bmatrix}\geq 0, \qquad \begin{bmatrix} \rho\\ \widetilde{\sigma}\\ \zeta \end{bmatrix}\geq 0. \tag{2.11}$$

Here $\widetilde{\mathbf{v}}=[\mathbf{v}^{(1)},\mathbf{v}^{(2)},\ldots,\mathbf{v}^{(m)}]$, $c_{\mathbf{v}}=[c_{\mathbf{v}}^{(1)},c_{\mathbf{v}}^{(2)},\ldots,c_{\mathbf{v}}^{(m)}]^T$, $\widetilde{n}=[n^{(j_1)},n^{(j_1)},\ldots,n^{(j_s)}]$, $c_n=[c_n^{(j_1)},c_n^{(j_2)},\ldots,c_n^{(j_s)}]^T$, $\widetilde{\beta}=[\beta^{(j_1)^T},\beta^{(j_2)^T},\ldots,\beta^{(j_s)^T}]^T$, $\widetilde{D}=[D^{(j_1)},D^{(j_2)},\ldots,D^{(j_s)}]$, $\lambda=[\lambda^{(j_1)},\lambda^{(j_2)},\ldots,\lambda^{(j_s)}]^T$, $\widetilde{\mu}=diag(\mu^{(j_1)},\mu^{(j_2)},\ldots,\mu^{(j_s)})^T$, $\Upsilon=\gamma\frac{1}{h}\left(\Theta^{(1)},\Theta^{(2)},\ldots,\Theta^{(m)}\right)^T$, $\Delta=\gamma\frac{1}{h}\left(\Phi^{(j_1)},\Phi^{(j_2)},\ldots,\Phi^{(j_s)}\right)^T$ and

$$\widetilde{E}=\begin{bmatrix} e^{(j_1)} & 0 & 0\cdots & 0\\ 0 & e^{(j_2)} & 0\cdots & 0\\ \vdots & \vdots & \vdots\vdots & \vdots\\ 0 & 0 & 0\cdots & e^{(j_s)} \end{bmatrix}$$

are the lumped LCP data, and $\mathcal{A}=\{j_1,j_2,\ldots,j_s\}$ are the active contact constraints. The vector inequalities in (2.11) are to be understood componentwise. We use the ˜ notation to indicate that the quantity is obtained by properly adjoining blocks that are relevant to the aggregate joint or contact constraints. The problem is called mixed LCP because it contains both equality and complementarity constraints.

To simplify the presentation, we have not explicitly included the dependence of the parameters in (2.10–2.11) on $q^{(l)}$. Also, $M^{(l)}=M(q^{(l)})$ is the value of the mass matrix at time $t^{(l)}$, and $k^{(l)}=k(t^{(l)},q^{(l)},v^{(l)})$ represents the external force at time $t^{(l)}$.

Choice of the active set $\mathcal{A}$ and collision detection. Most previous approaches have a simulate-detect-restart flavor (Anitescu and Potra, 1997; Baraff, 1993; Cremer and Stewart, 1989; Stewart and Trinkle, 1995). In these approaches, after the velocity is determined as a solution of the LCP, the simulation does not necessarily progress for the duration of the timestep if a collision is encountered. The simulation is stopped at the collision, the collision is resolved by using LCP techniques (Glocker and Pfeiffer, 1995; Anitescu and Potra, 1997), and the simulation is restarted. For such approaches, the active set is updated as a result of collision detection. If many collisions occur per unit of simulation, then there will be many costly updates that will interfere with the performance of the solver.

In the approach presented here, the active set is defined, with $\hat{\varepsilon}$ an apropriately chosen quantity, as

$$\mathcal{A}(q)=\left\{j|\Phi^{(j)}(q)\leq\hat{\varepsilon},\ 1\leq j\leq p\right\}. \tag{2.12}$$

In this case there is no need to stop the simulation if $\hat{\varepsilon}$ is appropriately chosen. A good guideline for this choice is $\hat{\varepsilon}=v_{\max}h$, where h is of the order of the expected size of the timestep and v_{max} is the expected range of the velocity. Since the definitions of the active sets are different, the results of computing with our definition of the active set and the simulate-detect-restart strategy are different. We can formally recover the simulate-detect-restart strategy in our approach by choosing $\gamma=0$ in (2.8) and (2.9).

Computationally, our approach is more appealing, since we solve only one LCP for fixed time-step h, which makes it more attractive for interactive simulation. An in-depth comparison of the two approaches is deferred to future research.

2.3 Pointed Friction Cone

To ensure that Δ and Υ do not destabilize the solution $v^{(l+1)}$, we require a certain constraint regularity to hold. This assumption is stated in terms of the properties of the friction cone.

We define the friction cone to be the portion in the velocity space that can be covered by feasible constraint interaction impulses, or

$$FC(q) = \left\{ t = \tilde{\nu} c_\nu + \tilde{n} c_n + \tilde{D}\tilde{\beta} \,\middle|\, c_n \geq 0,\ \tilde{\beta} \geq 0, \left|\left| \beta^{(j)} \right|\right|_1 \leq \mu^{(j)} c_n^{(j)},\ \forall j \in \mathcal{A} \right\}. \tag{2.13}$$

Clearly, the cone $FC(q)$ is a convex set.

Definition (Stewart, 2000): We say that the friction cone $FC(q)$ is pointed if it does not contain any proper linear subspace.

If the friction cone is not pointed, the configuration can get "stuck" . A good example of a nonpointed friction cone appears in a bidimensional slider-crank mechanism, with dry friction on both inside walls of the slider. If the slider is tight on its guiding rod, intuitively we see that it would get stuck.

From here on we assume that all encounteted configurations have a *uniformly* pointed friction cone. This assumption is essential in ensuring that the limits of the solutions of the time-stepping scheme (2.10)–(2.11) converge to a weak solution of the continuous problem (Stewart, 2000). In our case, this has two immediate consequences.

1. The mixed LCP (2.10)–(2.11) is guaranteed to have a solution (Pang and Stewart, 1999).
2. We have the following upper bound on the velocity solution of (2.10)–(2.11) (Anitescu and Hart, 2002)

$$\begin{aligned} {v^{(l+1)}}^T M^{(l)} v^{(l+1)} \leq {v^{(l)}}^T M^{(l)} v^{(l)} + h_l^2 {k^{(l)}}^T {M^{(l)}}^{-1} k^{(l)} \\ + 2h_l {v^{(l)}}^T k^{(l)} + c(q^{(l)}, \tilde{\mu}, M^{(l)})^2 \left|\left| \Delta_-^{(l)}, \Upsilon^{(l)} \right|\right|_\infty^2. \end{aligned} \tag{2.14}$$

The uniformly pointed friction cone assumption implies that the quantity $c(q^{(l)}, \tilde{\mu}, M^{(l)})$ is uniformly upper bounded by c_U during our simulation (Anitescu and Hart, 2002).

Here we used the notation $a_- = -\min\{a, 0\}$, where a is a real number. The quantitiy a_- is the negative part of the number a.

3 Analysis

Our main result concerns the behavior of the infeasibility of the noninterpenetration and the joint constraint. We define the measure of constraint infeasibility to be the maximum value of all infeasibilities of all individual geometrical constraints.

$$I(q) = \max_{1 \leq j \leq p, 1 \leq i \leq m} \left\{ \Phi_-^{(j)}(q), |\Theta^{(i)}(q)| \right\}. \tag{3.15}$$

To achieve our constraint stabilization results, we need two more assumptions to hold.

(D1) The mass matrix $M^{(l)} = M(q^{(l)})$ is constant and positive definite. We denote the constant mass matrix by M. This situation can be achieved by using the Newton-Euler formulation in body coordinates in three dimensions (Murray et al., 1993). In two dimensions, the same situation is achieved by using the world coordinates (Haug, 1989). This is mostly a simplifying assumption, as most results can be obtained without it.

(D2) The external force is continuous and increases at most linearly with the position and the velocity and is uniformly bounded in time. Hence,

$$k(t, v, q) = k_0(t, v, q) + f_c(v, q) + k_1(v) + k_2(q), \tag{3.16}$$

and there exists $c_K \geq 0$ such that

$$||k_0(t, v, q)|| \leq c_K,\ ||k_1(v)|| \leq c_K ||v||,\ ||k_2(q)|| \leq c_K ||q||. \tag{3.17}$$

Here $f_c(v, q)$ is the Coriolis force, which satisfies the following important property (Anitescu and Potra, 2002):

$$v^T f_c(v, q) = 0,\ \forall v, q. \tag{3.18}$$

Elastic forces are contained in k_2, whereas damping forces are contained in k_1.

Theorem 3.1. *Assume that the initial infeasibility is* 0*, or* $I(q^{(0)}) = 0$*. For fixed* $\gamma \in (0, 1]$ *and time-steps satisfying* $\frac{h_j}{h_l} \leq c_h$ *for any* $j \leq l$*, where* $c_h > 0$ *is a fixed constant, there exist a* V *and* H *such that whenever* $h_l \leq H$*, the velocity sequence is uniformly bounded over an arbitrary-length fixed finite interval ,* $v_l \leq V$*,* $\forall l$*.*

In addition*, there exist the parameters* C_1 *and* C_2 *that do not depend on the time-step and for which the geometrical constraint infeasibility satisfies*

$$I(q^l) \leq (1 - \gamma) I(q^{l-1}) + C_1 h_{l-1}^2 \left|\left| v^{(l)} \right|\right|^2 \leq C_2 \frac{1}{\gamma} \left(\max_{1 \ldots l} h_l \right)^2 V^2.$$

Proof In the following we develop several upper bounds that depend on positive parameters. For simplicity, we denote all the parameters by c_B.

The proof is based on (2.14), on the fact that $q^{(l+1)} = q^{(l)} + v^{(l+1)}$, and on the following observations.

1. We denote by

$$z_l = \left|\left|M^{-\frac{1}{2}} v^{(l)}\right|\right|, \quad w_l = \left|\left|q^{(l)}\right|\right|. \tag{3.19}$$

Using assumption (D2), we obtain that $v^{(l)^T} k^{(l)} \leq c_B(z_l + z_l^2 + z_l w_l)$, for some $c_B > 0$. From the definition of the infeasibility measure, of the active set $\mathcal{A}$ and of Δ and Υ in (2.10)–(2.11), we must have that $I(q^{(l)}) = \frac{h_l}{\gamma} \left|\left|\Delta_-^{(l)}, \Upsilon^{(l)}\right|\right| \infty$. When used with (2.14) and the last inequality, this implies that

$$\begin{aligned} z_{l+1}^2 \leq z_l^2 + h_l^2 k^{(l)} M^{(l)-1} k^{(l)} \\ +2c_B h_l (z_l + z_l^2 + z_l w_l) + c_U \gamma^2 \left(\tfrac{I(q^{(l)})}{h_l}\right)^2. \end{aligned} \tag{3.20}$$

2. Using (2.9) and the fact that $q^{(l+1)} = q^{(l)} + h_l v^{(l+1)}$, we obtain, using Taylor's theorem, that, if $j \in \mathcal{A}$, we have that

$$\begin{aligned} \Phi^{(j)}(q^{(l+1)}) &\geq \Phi^{(j)}(q^{(l)}) \\ &\quad + h_l n^{(j)^T}(q^{(l)}) v^{(l+1)} + c_{2D} h_l^2 \left|\left|v^{(l+1)}\right|\right|^2 \\ &\geq (1-\gamma)\Phi(q^{(l)}) + c_{2D} h_l^2 \left|\left|v^{(l+1)}\right|\right|^2, \end{aligned}$$

where c_{2D} is an upper bound on the size of the second derivative of Φ. Similarly, using (2.8), we obtain the following inequality for the equality constraints.

$$\begin{aligned} \left|\Phi^{(j)}(q^{(l+1)})\right| &\geq \left|\Phi^{(j)}(q^{(l)}) + h_l n^{(j)^T}(q^{(l)}) v^{(l+1)}\right| \\ &\quad + c_{2D} h_l^2 \left|\left|v^{(l+1)}\right|\right|^2 \\ &= (1-\gamma)\left|\Phi(q^{(l)})\right| + c_{2D}^2 h_l^2 \left|\left|v^{(l+1)}\right|\right|^2. \end{aligned}$$

3. If the time-step h_l is sufficiently small, then the only infeasible constraints at step $l+1$ are the ones that belong to $\mathcal{A}$. This result follows from the choice of $\hat{\varepsilon} > 0$ from the definition of the active set $\mathcal{A}$, and from the fact that the velocity is bounded. As a result, we can use the definition of $I(q^l)$ to get, from the previously displayed equations that

$$I(q^{(l+1)}) \leq (1-\gamma) I(q^{(l)}) + c_{2D} h_l^2 \left|\left|v^{(l+1)}\right|\right|^2. \tag{3.21}$$

The argument, as we presented it, is circular. We need a bounded velocity to state (3.21). In turn, (3.21) is needed to prove that the velocity is bounded using (3.20). This can be fixed by proving (3.21) simultaneously with the bounded velocity property, but this leads to an exceedingly technical proof (Anitescu and Hart, 2002). So we simply assume (3.21).

Using the position recursion equation $q^{(l+1)} = q^{(l)} + h_l v^{(l+1)}$, the equation (3.19), and the triangle inequality, we obtain that, for some appropriate parameter c_B,

$$w_{l+1} \leq w_l + c_B h_l z_{l+1}. \tag{3.22}$$

We denote

$$\hat{w}_l = \max_{j=0,1,\ldots,l} w_j, \quad \hat{z}_l = \max_{j=0,1,\ldots,l} z_j, \quad \hat{h}_l = \max_{j=0,1,\ldots,l} h_j,$$

Note that $\hat{w}_l$, $\hat{z}_l$ and $\hat{w}_l$ are nonnegative, increasing sequences. An immediate consequence from assumption (D1) and (3.21) is that

$$I(q^{(l+1)}) \leq (1-\gamma) I(q^{(l)}) + c_{2D} c_B h_l^2 z_{l+1}^2,$$

for an appropriately chosen c_B. This implies, in turn, that

$$\begin{aligned} I(q^{(l+1)}) &\leq c_{2D} c_B \textstyle\sum_{j=1}^{l+1} (1-\gamma)^{l+2-j} h_l^2 z_j^2, \\ &\leq \tfrac{c_{2D} c_B \hat{h}_l^2}{\gamma} \hat{z}_{l+1}^2 \leq \tfrac{c_{2D} c_B c_h^2 h_{l+1}^2}{\gamma} \hat{z}_{l+1}^2. \end{aligned} \tag{3.23}$$

If we denote by $c_F = c_{2D} c_B c_h^2 c_U$ and we replace the last inequality in (3.20), with $l+1$ replaced by l, we obtain that

$$\begin{aligned} z_{l+1}^2 \leq z_l^2 + h_l^2 k^{(l)} M^{(l)-1} k^{(l)} \\ +2c_B h_l (z_l + z_l^2 + z_l w_l) + c_F h_l^2 \hat{z}_l^4. \end{aligned} \tag{3.24}$$

Note that the bound on z_{l+1} and thus on velocity is independent of $\gamma \in (0,1]$.

It is immediate that if we replace z_l with $\hat{z}_l$, and w_l with $\hat{w}_l$ in (3.22) and (3.24), the inequalities will continue to hold. This is a typical technique from the analysis of stability of numerical solutions to ordinary differential equations (Atkinson, 1989, Theorem 6.6).

But then the resulting inequalities are a particular case of the ones in the statement of [Theorem II.2](Anitescu and Hart, 2002). Applying that particular result implies that there exist $H > 0$ and $V > 0$ such that, whenever $h_l \leq H$ for all l and $\sum_{l=0}^{N} h_l = T$, where T is any fixed time interval, then $v_l \leq V$ for all l. This proves the first part of the claim.

The second part of the claims follows from (3.21) by using assumption (D1) and (3.19) and (3.23). $\diamond$.

Why does this show that it is constraint stabilization? We can see that the effect of the constraint infeasibility at each step l is dampened by $(1-\gamma)$ per step as time progresses and the infeasibility depends mostly on the velocity values near time l. In particular, if the velocity drops to 0, then the infeasibility eventually drops to 0. This effect is not seen in unstabilized schemes that base their constraint satisfaction on small time steps. This effect is most visible when $\gamma = 1$, when the infeasibility at step l depends strictly on the value of v^l, as was also shown in (Anitescu and Hart, 2002).

The theorem also guarantees that the infeasibility will go to 0 as $\max_l h_l^2$. In addition, it seems to indicate that larger γ results in faster constraint stabilization as soon as $\gamma \leq 1$.

4 Numerical Results

In this section we demonstrate constraint infeasibility behavior when we apply the method described in this work.

In the first, two-dimensional, example, we simulate an elliptic body dropped on a tabletop. The length of its axes are 8 and 4. The body is dropped from a height of 8 with respect to its center of mass and with an angular velocity of 3. The friction coefficient is 0.3. In Figure 1 we present ten frames of the simulation, which is run with a constant time step of 50 milliseconds. In Figure 2 we present a comparison of the constraint infeasibility between the unstablilized and stabilized version of our algorithm, for different values of γ.

From Figure 2 we see that $\gamma = 0$ does result in the constraint infeasibility's increasing steadily. On the other hand we see that $\gamma \in (0,1]$ results in constraint stabilization, as predicted by Theorem 3.1. In addition, larger γ results in faster constraint stabilization. We also see the exponential drop in infeasibility following an event, which is consistent with the recursion of the infeasibility presented in Theorem 3.1.

In the second example, we present a robotic grasp simulation that implements the method described in this work. In our framework, we need to have access to the mappings $\Phi^{(j)}$ that quantify the signed distance function. While there is well-defined methodology to compute the signed distance function between any two bodies that may or may not interpenetrate (Kim et al., 2002), there is substantially more software that computes the Euclidean distance function only if the bodies do not interpenetrate and returns a message if the bodies interpenetrate. To work with such software in our grasp simulator, we have defined a "protective layer" of 5 mm around the body, and we shift the value of the distance function by 5 mm. This allows us to use the Euclidean distance function until the interpenetration (as measured by the shifted distance function) reaches 5 mm, at which point we are unable to continue the simulation. More details and parameters of the simulation can be found in (Miller and Christensen, 2002).

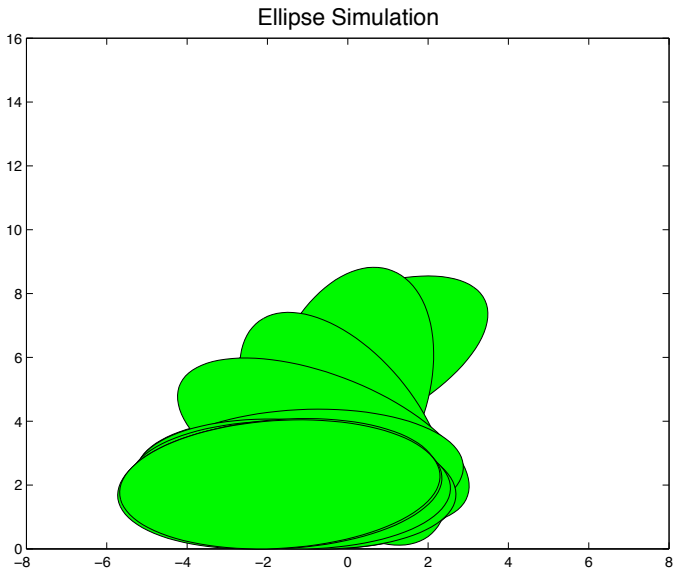

Figure 1. Ten frames of an ellipse on a tabletop simulation.

The situation we simulate is represented in Figures (5)–(12). The configuration consists of a glass that is within the reach of a Bartlett hand that starts to close. There is friction at all contacts, but, in this particular case, the friction at the hand is too small to close the grasp. The simulation is run with a constaint time step of 2.5 ms. In Figure 3 we present the contact constraint infeasibility, whereas in Figure 4 we present the total (joint and contact) constraint infeasibility, measured in the $||\cdot||_\infty$, just as we did in the definition of $I(q^{(l)})$.

For $\gamma = 0$, the constraint infeasibility kept increasing until we reached the 5 mm limit defined above and the simulation had to stop. When we ran the simulation with $\gamma = 0.2$ and $\gamma = 1$, the constraint infeasibility drift was arrested, just as predicted by Theorem 3.1. In addition, the constraint infeasibility behavior for $\gamma = 0.2$ was consistent with an exponential drop in infeasibility after an event, much as suggested by the recursion in Theorem 3.1. This is visible especially in the joint infeasibility behavior in Figure 3. We also see that larger $\gamma = 1$ does result in faster constraint stabilization, also as predicted by Theorem 3.1.

From Figure 4 we observe that choosing $\gamma = 1$, does not necessarily result in the smallest constraint infeasibility value, though constraint stabilization is rapidly achieved (the fastest of any choice). Hence, it may be beneficial to explore an adaptive choice of γ, which we plan to do in future research.

5 Conclusions and Future Work

We presented a time-stepping scheme for multibody dynamics with joints, contact, and friction that stabilizes constraint infeasibility while solving only one linear complementarity prob-

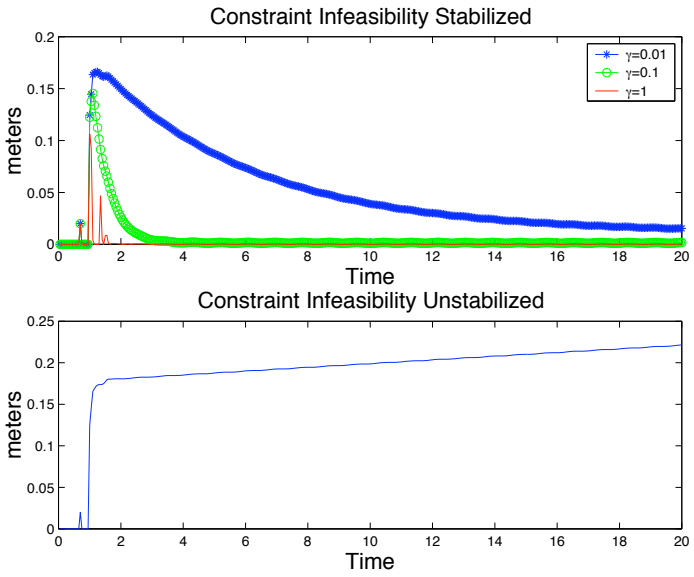

Figure 2. Ellipse simulation: Comparison of the constraint infeasibility between the unstabilized method and the stabilized method.

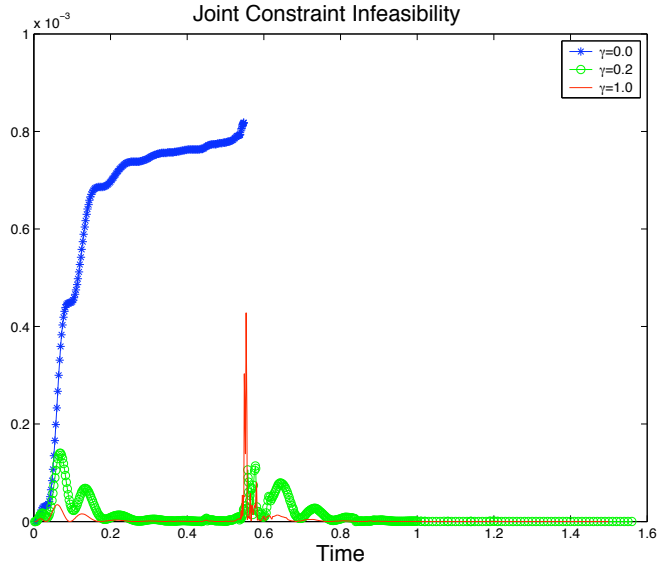

Figure 3. Joint constraint infeasibility for the robot hand simulation.

lem per step. The constraint stabilization effect is both proved in Theorem 3.1 and demonstrated by a two-dimensional and a three-dimensional example.

Future work needs to address the problem of incorporating partially elastic collisions that may deteriorate the energy bound (2.14) based on which the stabilization result is proved. It is also important to extend these results to nonsmooth shapes, which abound in practical applications. Finally we will study ways to

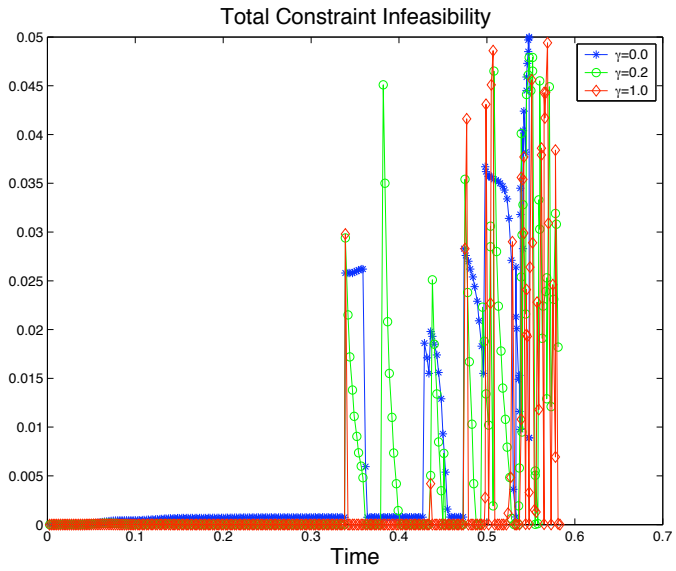

Figure 4. Total constraint infeasibility for the robot hand simulation.

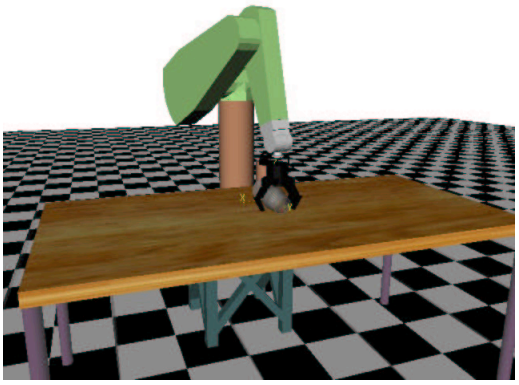

Figure 5. Time=0.0050.

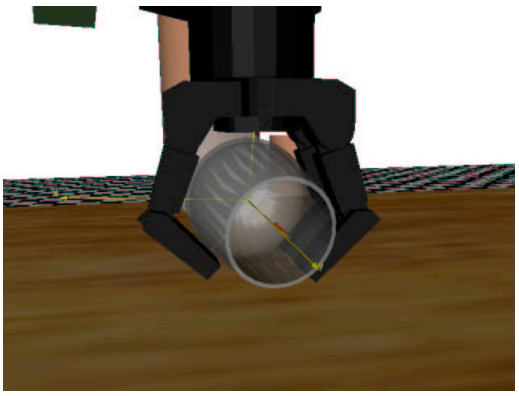

Figure 6. Time=0.4781.

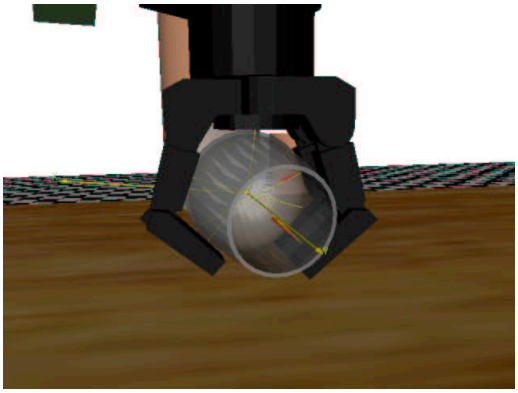

Figure 7. Time=0.5103.

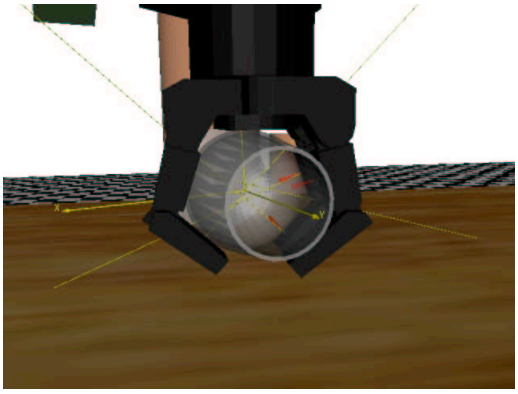

Figure 8. Time=0.5425.

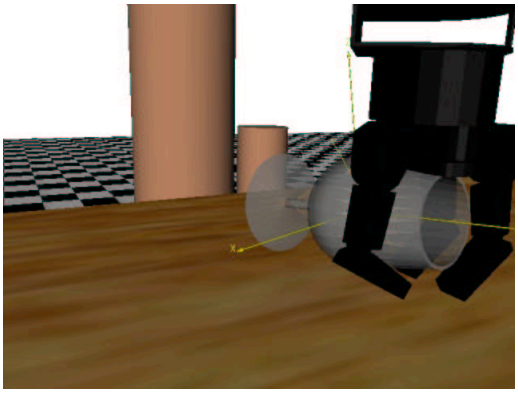

Figure 9. Time=0.5782.

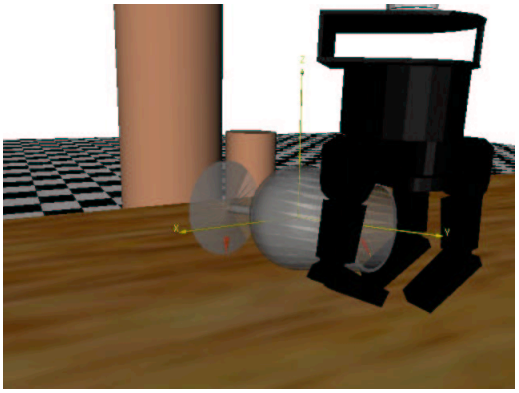

Figure 10. Time=0.6148.

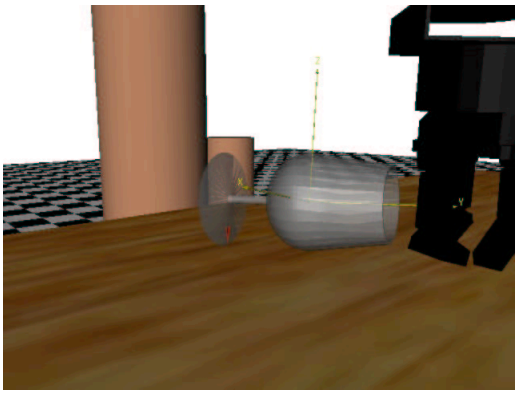

Figure 11. Time=0.6586.

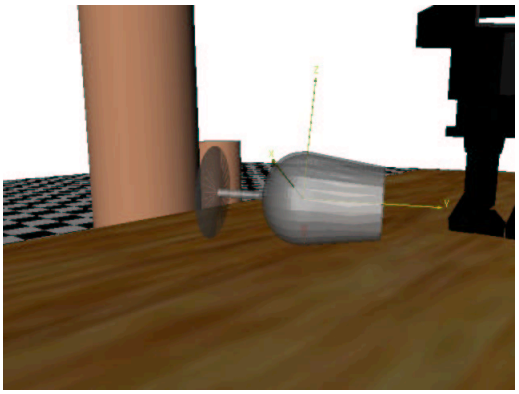

Figure 12. Time=0.6956.

adaptively choose γ.

Acknowledgments

We thank Michael Ferris and Todd Munson for providing and maintaining PATH (Munson, 2000; Dirkse and Ferris, 1995), a package for solving general linear complementarity problems. This work was performed under Contract No. W-31-109-ENG-38 with the U.S. Department of Energy (Mihai Anitescu) and under a CRDF award from the University of Pittsburgh (Mihai Anitescu and Gary D. Hart).

REFERENCES

Anitescu, M., and Hart, Gary D. "A constraint-stabilized time-stepping scheme for multi-body dynamics with contact and friction", Preprint ANL/MCS-P1002-1002, Mathematics and Computer Science Division, Argonne National Laboratory, 2002. Available at *http://www.mcs.anl.gov/~anitescu/PUBLICATIONS/reports.html*.

Anitescu, M., and Potra, F. A., "A time-stepping method for stiff multibody dynamics with contact and friction", *Int. J. Numerical Methods in Engineering* **55**(7), 753–784, 2002.

Anitescu, M., and Potra, F. A., "Formulating rigid multi-body-dynamics with contact and friction as solvable linear complementarity problems", *Nonlinear Dynamics* **14**, 231–247, 1997.

Anitescu, M., Stewart, D., and Potra, F. A., "Time-stepping for three-dimensional rigid body dynamics", *Computer Methods in Applied Mechanics and Engineering* **177**(3–4), 183–197, 1999.

Anitescu, M., Cremer, J., and Potra, F. A., "Formulating 3D contact dynamics problems", *J. Mech. Struct. Mach.* **24**(4), 405–437, 1996.

Ascher, U., Chin, H., and Reich, S. "Stabilization of DAEs and invariant manifolds", *Numerische Mathematik*, **67**, 131–149, 1994.

Ascher, U., and Petzold, L. *Computer Methods for Ordinary Differential Equations and Differential-Algebraic Equations*, SIAM, Philadelphia, 1998.

Ascher, U., Chin, H., Petzold, L., and Reich, S. "Stabilization of constrained mechanical systems with DAEs and invariant manifolds", *J. Mech. Struct. Mach*, **23**, 135-158, 1995.

Atkinson, K. E., *An Introduction to Numerical Analysis*, John Wiley and Sons, New York, 1989.

Baraff, D., "Issues in computing contact forces for non-penetrating rigid bodies", *Algorithmica* **10**, 292–352, 1993.

Cline, M., *Rigid Body Simulation with Contact and Constraints*, M.S. thesis, Department of Computer Science, University of British Columbia, 2002.

Cremer, J. F., and Stewart, A. J. "The architecture of Newton, a general purpose dynamics simulator", *Proceedings of the IEEE International Conference on Robotics and Automation*, 1989, pp. 1806–1811.

Dirkse, S. P., and Ferris, M. C., "The PATH solver: A non-monotone stabilization scheme for mixed complementarity problems", *Optimization Methods and Software* **5**, 123–156, 1995.

Donald, B. R., and Pai, D. K. "On the motion of compliantly connected rigid bodies in contact: a system for analyzing designs for assembly", *Proceedings of the Conf. on Robotics and Automation*, 1990, pp. 1756–1762.

Glocker, C., and Pfeiffer, F. "An LCP-approach for multibody systems with planar friction", *Proceedings of the CMIS 92 Contact Mechanics Int. Symposium, Lausanne, Switzerland,*, 1992, pp. 13–20.

Haug, E. J., *Computer Aided Kinematics and Dynamics of Mechanical Systems*, Allyn and Bacon, Boston, 1989.

Kim, Y. J., Lin, M. C., and Manocha, D., "DEEP: Dual-space expansion for estimating penetration depth between convex polytopes", *Proceedings of the IEEE International Conference on Robotics and Automation,* 2002.

Lo, G., Sudarsky, S., Pang, J.-S., and Trinkle, J., "On dynamic multi-rigid-body contact problems with Coulomb friction," *Zeitschrift fur Angewandte Mathematik und Mechanik* **77**, 267–279, 1997.

Miller, A., and Christensen H. I., "Implementation of multi-rigid-body dynamics within a robotics grasping simulator", preprint, 2002. Available at *http://www.cs.columbia.edu/~amiller/graspit/index.html*.

Glocker, C., and Pfeiffer, F., "Multiple impacts with friction in rigid multi-body systems", *Nonlinear Dynamics* **7**, 471-497, 1995.

Munson, T. S., *Algorithms and Environments for Complementarity*, Ph.D. thesis, Department of Computer Science, University of Wisconsin-Madison, 2000.

Murray R. M., Li, Z., and Sastry, S. S., *Robotic Manipulation*, CRC Press, Boca Raton, FL, 1993.

Pang, J.-S., and Stewart, D.E., "A unified approach to frictional contact problems", *Int. J. Engineering Science*, **37**, 1747–1768, 1999.

P. Song, P. Kraus, V. Kumar, and P. Dupont, "Analysis of rigid-body dynamic models for dimulation of systems with frictional contacts" *J. Applied Mechanics* **68(1)**, 118-128, 2001.

Stewart, D., "Rigid-body dynamics with friction and impact", *SIAM Review* **42** (1), 3–29, 2000.

Stewart, D. E., and Trinkle, J. C., "An implicit time-stepping scheme for rigid-body dynamics with inelastic collisions and Coulomb friction", *International J. Numerical Methods in Engineering* **39**, 2673-2691, 1996.